

Characterization and Toxicological Assessment of Iron and Zinc Nanoparticles in Male Wistar Rats

Martina A. Gamit^{1*}, Manoj N. Brahmabhatt², Prakrutik P. Bhavsar¹, Bhupendra C. Parmar¹, Mounil Mankan³, Ghanshyam B. Patil³

ABSTRACT

Iron deficiency anaemia (IDA) is often studied using rat models to better understand the condition and evaluate treatment options. In this study an *in vivo* rat model of IDA was developed by inducing dietary iron deficiency anaemia (IDA) by offering iron-deficient diet over a period of 8-weeks to male Wistar rats as evidenced by a significant reduction in haemoglobin levels to below 9 g/dL, thereby providing a robust framework. This study explored the formulation and characterization of iron and zinc nanoparticles (100 nm and 71 nm, respectively). Adult Wistar rats (n=24) were distributed into three equal groups for treatment trial of 56 days. One group kept as control (T1) received double distilled water, while treatment groups received ionic form (T2) of 0.1 M solution each of ferric chloride hexahydrate and zinc sulphate heptahydrate, and nanoparticle forms (T3) of iron (20 mg/d) and zinc (10 mg/d doses). Acute toxicity in the nanoparticle-treated group T3 led to 100 % mortality within 24 h with severe histopathological alterations in vital organs like liver, kidneys, spleen, heart and testes, while in ionic form T2 group subacute toxicity occurred, which was assessed over 56 days with very mild cellular changes or structures almost towards normal control group. The findings emphasized the need for cautious evaluation of zinc and iron nanoparticles in therapeutic applications.

Keywords: Characterization, Iron deficiency anaemia, Nanoparticles, Rat model, Toxicological assessment.

Ind J Vet Sci and Biotech (2025): 10.48165/ijvsbt.21.5.06

INTRODUCTION

Micronutrients, including vitamins and minerals, are essential for various physiological functions and overall health. Deficiencies in micronutrients like iron, zinc, manganese, and selenium can lead to serious health issues such as weakened immunity, infections, anaemia, and cognitive impairment. Iron is crucial for oxygen transport, DNA synthesis, metabolism, and immune function, with deficiencies causing anaemia, fatigue, and weakness. Zinc, the second most abundant trace mineral, is vital for growth, immunity, reproduction, wound healing, and cellular functions. Ensuring adequate intake of these micronutrients is essential for preventing deficiencies and maintaining overall well-being (Chen, 2023). Anaemia is a condition where the blood ability to carry oxygen is reduced due to low haemoglobin levels or insufficient red blood cells. It indicates poor nutrition and overall health, significantly affecting women and children. Common causes include iron, folate, vitamin B₁₂, and vitamin A deficiencies, as well as genetic disorders, viral infections like HIV, and parasitic infections (Chaparro and Suchdev, 2019; Dubey *et al.*, 2020).

Nanoparticles (NPs) are ultrafine units with dimensions measured in nanometers (1 nm = 10⁻⁹ metre) and their lengths are ranging from 1-100 nm (Ijaz *et al.*, 2020). Upon discovery that the nanosize of particles might affect their physiochemical properties, the scientists have become more focused on the significance of NPs materials. Rat models of iron deficiency anaemia (IDA) are essential for researching the condition and assessing possible therapies. Usually, these models are created by causing rats to become iron

¹Department of Livestock Products Technology, College of Veterinary Science and Animal Husbandry, Kamdhenu University, Anand-388001, Gujarat, India

²Department of Veterinary Public Health and Epidemiology, College of Veterinary Science and Animal Husbandry, Kamdhenu University, Anand-388001, Gujarat, India

³Department of Nanotechnology, Anand Agricultural University, Anand-388110, Gujarat, India

Corresponding Author: Martina A. Gamit, Department of Livestock Products Technology, College of Veterinary Science and Animal Husbandry, Kamdhenu University, Anand-388001, Gujarat, India. E-mail: drmartina@kamdhenuuni.edu.in

How to cite this article: Gamit, M. A., Brahmabhatt, M. N., Parmar, B. C., Bhavsar, P. P., Mankan, M., & Patil, G. B. (2025). Characterization and Toxicological Assessment of Iron and Zinc Nanoparticles in Male Wistar Rats. *Ind J Vet Sci & Biotech*, 21(5), 29-34.

Source of support: Nil

Conflict of interest: None

Submitted 11/03/2025 **Accepted** 06/05/2025 **Published** 10/09/2025

deficient, either by giving them meals low in iron or by using particular chemicals. This study reports the development and evaluation of *in vivo* iron deficiency anaemia model in rats and characterization and toxicological assessment of iron and zinc nanoparticles in male Wistar rats as well.

MATERIALS AND METHODS

Synthesis of Iron and Zinc Nanoparticles

Iron nanoparticles were synthesized as per Zambri *et al.* (2019) using a 0.1 M magnetically stirred ferric chloride

hexahydrate solution (27.030 g in 1 L distilled water) with slight modifications. For the reaction, 960 mL of this solution was combined with 40 mL neem extract, mixed thoroughly, and heated in a 90 °C water bath for 1 h, inducing a color change from light red to dark brown, giving the resultant solution having the nanoparticles of ferric oxide.

Similarly, zinc nanoparticles were synthesized using a 0.1 M magnetically stirred zinc sulphate heptahydrate solution (28.756 g in 1 L distilled water), added with 1 M NaOH solution dropwise to adjust the pH to 8.5 while continuously stirring. The mixture was filtered, washed, and the pellet was dispersed in 125 mL distilled water and 875 mL of 0.5% carboxymethyl cellulose solution, stirred for 30 min. The final mixture was homogenized using a GEA Panda Plus Lab Homogenizer 2000, yielding ZnO nanoparticles for further study (Annonymous, 2018).

For the bulk ionic form of iron and zinc, the plain 0.1 M solution each of ferric chloride hexahydrate and zinc sulfate heptahydrate, respectively, were used without further adding anything.

Characterization of the Size and Zeta Potential of Nanoparticles

Dynamic light scattering (DLS), performed using a Zetasizer Nano ZS90 (Malvern, UK), was employed to determine the particle size distribution and zeta potential of nanoparticle suspensions, following the method of Omar *et al.* (2014). A 633 nm helium-neon laser illuminated the sample, and scattered light was detected at a fixed angle of 173°, allowing calculation of hydrodynamic diameter via the Stokes-Einstein equation (Zaman *et al.*, 2016). The mean particle size, or Z-average diameter (d_x), was based on light intensity from polydisperse samples. DLS instruments measure particles ranging from 2-6 µm. Suspensions were injected into pre-rinsed, single-use polystyrene vials and analyzed for 5 min at 25 °C.

Characterization of Nanoparticles by Atomic Absorption Spectrometry (AAS) and Fourier Transform Infrared Spectroscopy (FTIR)

The concentrations of iron (Fe) and zinc (Zn) were quantified using Atomic Absorption Spectrometry (AAS) in the Department of Micronutrients at Anand Agricultural University, Anand. Standard solutions were used to establish a linear calibration curve. The concentrations derived from the absorbance measurements were determined using the intersection of the calibration graph. Metal concentrations were subsequently used to prepare the respective doses.

Nanoparticle suspensions were dried in a hot air oven at 60 °C for 24 h and then analyzed using Fourier Transform Infrared Spectroscopy (FTIR) with a Perkin Elmer instrument (Waltham, Massachusetts, USA) at a resolution of 4 cm⁻¹. Approximately 2 mg of each sample was placed on the stage and scanned across a wavenumber range of 400-4000 cm⁻¹ to assess chemical bonds and surface structure.

Experimental Animals and Induction of Anaemia

The experiment was conducted in a Small Animal House, Veterinary College, Kamdhenu University, Anand (Gujarat, India). For the experiment, 24 male Wistar rats (*Ratus norvegicus*) (74-78 g) were obtained from Cadila Pharmaceuticals Ltd., Dholka (Gujarat, India). The Institutional Animal Ethics Committee approved the study (approval No. GVC/LPT/366/2022). All laboratory animals were acclimatized for three days to the new diet and environment within the laboratory facility.

Rats were individually weighed and divided into three equal groups of uniform body weights (74-78 g). The rats were housed in polypropylene cages in an environmentally controlled room at 22 ± 2°C. Relative humidity was maintained at a minimum of 30% and a maximum of 70%, except during room cleaning when it was around 50-60%. Throughout the study period, the rats were provided with a 12-h light/dark cycle. They were fed *ad libitum* with standard pelleted feed, manufactured by VRK's Iron deficient Rat/Mice Pelleted Feed, and double distilled water was also provided *ad libitum* for the rats to develop an *in vivo* rat model of iron deficiency anaemia (IDA) over an 8-week period. Haemoglobin levels were monitored weekly, aiming for reduction in haemoglobin below 9 g/dL as a decline in haemoglobin (Hb) levels serves as a critical indicator of IDA, particularly in rat models (Suva and Tirgar, 2023). The study successfully established a reliable rat model of IDA within 8-weeks, providing a valuable framework for further studies.

Preparation of the Doses and Dosing of Rats for Toxicity Assessments

The preparation of dose entailed the combination of the appropriate concentration of the concentrated solution at the desired dose/treatment level to obtain the desired effect. The IDA rats were subjected to three treatments, the rats of treatment/group 2 and 3 were restrained using the scruff method and were administered iron and zinc in their ionic form at dosage rates of 20 mg/d and 10 mg/d, respectively (T2) for 8-weeks. Similarly, the nano form of iron and zinc was administered at the same dosage rates of 20 mg/d and 10 mg/d, respectively (T3). All administrations were conducted orally via oral gavage using 2 mL disposable syringe with a blunt crop feeding needle. The rats of treatment/group 1 (control, T1) received only distilled water (Table 1). To prevent the dose from being aspirated into the respiratory tract, the rat was held vertically during oral gavage.

To our surprise, acute toxicity was observed in the group administered with a very high dose of iron and zinc nanoparticles (T3), resulting in mortality of all the rats within 24 h of first dosing, while in group T2, subacute toxicity was observed over a period of 56 days. Hence, post-mortem examination and collection of samples were done on death of animals in group T3, while the rats of T2 (ionic form) and T1 (control) groups were euthanized at the end of



Table 1: Grouping, treatments and dosing of ionic forms and nanoparticle forms of iron and zinc to star rats

Groups	Animals	Treatments	Iron dose (mg/d)	Zinc dose (mg/d)	Route
Control	8	Distilled water (T1)	-	-	Oral
Anaemic Group-I	8	Higher dose Ionic form (T2)	20	10	Oral
Anaemic Group-II	8	Higher dose Nano form (T3)	20	10	Oral

experiment (day 56) and the tissues of organs like liver, kidney, spleen, heart, and testis were collected in 10% formalin for histopathological examination adopting standard section cutting and staining procedures.

RESULTS AND DISCUSSION

Characterization of Iron and Zinc Nanoparticles

In this study, iron and zinc nanoparticles were characterized using Dynamic Light Scattering (DLS), Zeta potentiometry, Atomic Absorption Spectrometry (AAS), and Fourier-Transform Infrared Spectroscopy (FTIR) to assess particle size, distribution, polydispersity index, functional groups, and absorption spectra. DLS analysis with a Zetasizer Nano ZS90 revealed average hydrodynamic diameters of 100 nm for iron and 71 nm for zinc nanoparticles. Both exhibited monodispersity with a polydispersity index (PDI) of 0.26. These findings aligned with previous reports, including Le *et al.* (2022) and Nahari *et al.* (2022) for iron nanoparticles (45-100 nm), and Kumar *et al.* (2020) for zinc nanoparticles (58.5 nm) synthesized via direct precipitation.

The stability of iron (Fe) and zinc (Zn) nanoparticles was assessed via Zeta potential measurements. Zinc nanoparticles exhibited a zeta potential of 17 mV, indicating a net negative surface charge. Zeta potential, reflecting the electrokinetic potential at the particle's diffuse boundary, is a critical indicator of colloidal stability. Higher absolute zeta potential values suggest stronger repulsive forces between particles, reducing aggregation. Typically, values exceeding ± 30 mV denote stable suspensions (Ostolska and Wisniewska, 2014).

The concentrations of iron (Fe) and zinc (Zn) were quantified using Atomic Absorption Spectrometry (AAS) as 2454 ppm and 2521 ppm for Fe and Zn Nano form, and 3631 ppm and 4396 ppm for Fe and Zn ionic form, respectively. These metal concentrations were subsequently used to prepare the respective doses.

The FTIR spectrum of iron nanoparticles showed key peaks at 3219.06 cm^{-1} (O-H stretching), 1615 cm^{-1} (C=C stretching), and several lower wavenumber bands at 853.05 , 666.97 , and 474.28 cm^{-1} corresponding to Fe-O stretching vibrations, indicating the presence of iron oxide. These findings aligned with those of Kulkarni *et al.* (2020), who reported similar peaks for green-synthesized hematite nanoparticles, and Tyagi *et al.* (2023), who observed characteristic O-H and Fe-O bands in superparamagnetic iron oxide nanoparticles (SPIONs).

The FTIR spectrum of zinc nanoparticles exhibited characteristic peaks corresponding to specific functional groups: 3400.96 cm^{-1} (O-H stretching), 1637.15 cm^{-1} (C=C stretching), 1474.70 cm^{-1} (C-H bending), 1119.77 cm^{-1} (C-O stretching), and 965.06 cm^{-1} (Zn-O stretching), confirming the metal oxide nature of the nanoparticles. These findings were consistent with those of Kumar *et al.* (2020) and Prajapati (2024), who reported similar peak positions in FTIR analyses of ZnO nanoparticles synthesized using plant extracts.

Toxicity Assessments through Histopathology

The rats of iron deficiency anaemia (IDA) model were included in three distinct treatment groups. The negative control group (T1) received double-distilled water, while the other two groups were administered very high doses of iron and zinc in ionic form (T2), and in nano form (T3), respectively. Acute toxicity was observed in the group T3 administered with a very high dose of iron and zinc nanoparticles, resulting in mortality of all rats within 24 h of administration of first dose. In contrast, subacute toxicity was observed in group T2 that received very high dose of iron and zinc in ionic form, which was assessed over a period of 56 days.

In the present study, histopathological examination of liver tissue revealed normal architecture characterized by well-organized hepatocyte plates, small portal tracts centrally located, and terminal hepatic venules positioned peripherally in both the control group (T1) and the ionic form group (T2) (Fig. 1) and in the group receiving the very higher dose of iron and zinc nanoparticles (T3) infiltration of inflammatory cells in the portal region and dilation of the portal vessels was observed (Fig. 2). The present findings in the control group (T1) are consistent with the results of Thakur *et al.* (2019), who reported that the liver exhibited normal histoarchitectural features.

Histopathological examination of the kidneys demonstrated normal architecture, characterized by structurally intact glomeruli with normal cellularity, maintained integrity of Bowman's capsules, and renal tubules lined by uniform cuboidal epithelial cells, with no histological evidence of cellular degeneration or necrosis in both the control group (T1) and the ionic form group (T2) (Fig. 3). In the very higher dose iron and zinc nanoparticles group (T3), histopathological examination of kidneys revealed evidence of tubular degeneration localized within the cortical region (Fig. 4). The findings in the control group (T1) were consistent

with the results of Thakur *et al.* (2019), who reported that the kidneys exhibited normal histoarchitectural features.

The histopathological examination of the spleen revealed a normal architectural pattern, with well-preserved white and red pulp structures in groups T1 and T2 (Fig. 5). The very high dose group of iron and zinc nanoparticles (T3) caused depletion of the white pulp (Fig. 6). The findings in the control group (T1) were consistent with the results of Thakur *et al.* (2019), who reported normal spleen structure in their study.

In the present study, histopathological examination of the heart revealed striated, branched, cardiac muscle fibers and interconnected by intercalated discs in all treatment groups exhibited normal cardiac structure, with no significant structural abnormalities, which is consistent with the observations made by Yun *et al.* (2015). Thakur *et al.* (2019), and Bhavsar (2022), all of whom reported a normal structure of heart in their respective investigations.

Histopathological examination of the testes revealed normal tissue architecture including the seminiferous tubules, interstitial cells, and other components of the testes,

appeared to be intact and healthy under the microscope in rats of T1 and T2 groups (Fig. 7). The results observed in T1 and T2, aligned closely with the findings reported by Bhavsar (2022). The group treated with the very high dose of iron and zinc nanoparticles (T3) revealed a significant loss of germ cells within the lumen of the seminiferous tubules (Fig. 8), which aligned with the results of Rehman *et al.* (2024), who investigated the effects of zinc oxide nanoparticles (ZnO-NPs) on rat testes. Their study demonstrated that exposure to a medium dose (20 mg/kg body weight) of ZnO-NPs resulted in moderate histological alterations, including vacuolation, Sertoli cell destruction, necrotic detachment of cells, germ cell loss within the seminiferous tubules, and congestion of Sertoli cells, while at a higher dose of 30 mg/kg body weight, the observed effects were more severe, with significant germ cell necrosis, vacuolation, edema, germ cell loss in the lumen of the seminiferous tubules, degeneration of seminiferous tubules, coagulative necrosis, epithelial apoptosis, and desquamation of spermatogenic cell.

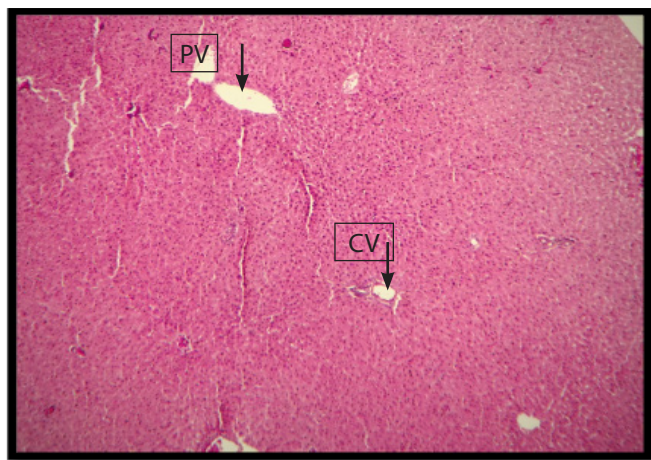


Fig. 1: Normal histological structure of liver (PV- Portal vein, CV- Central vein) in group 1 and 2 rats (40X)

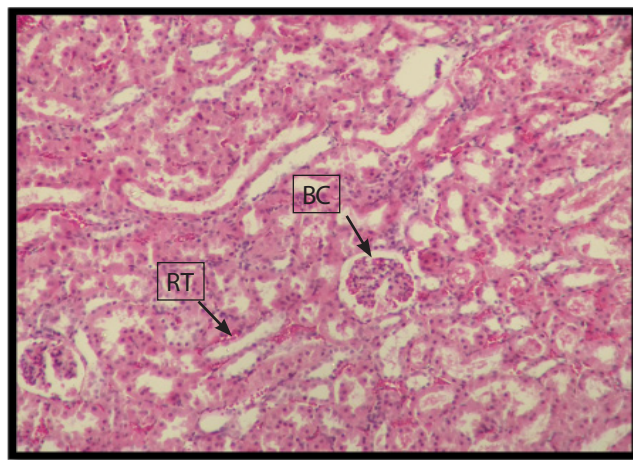


Fig. 3: Normal histological structure of kidney (BC- Bowman's capsules, RT- Renal Tubules) in group 1 and 2 rats (100X)



Fig. 2: Inflammatory cell infiltration in the portal region of liver (PV Portal vein) in group 3 rats (40X)

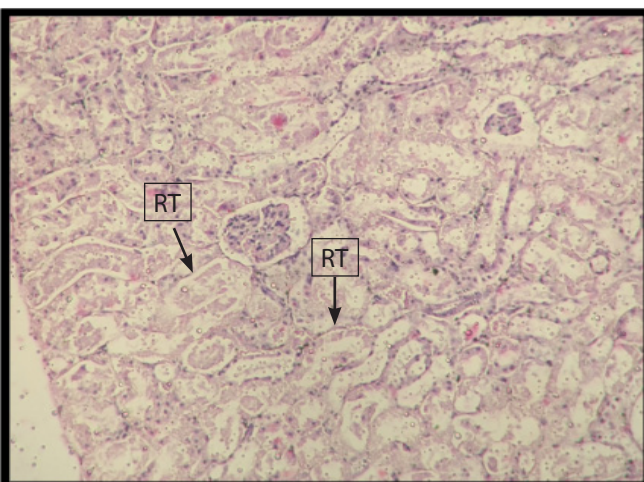


Fig. 4: Tubular degeneration in kidney (RT- Renal Tubules) in group 3 rats (100X)

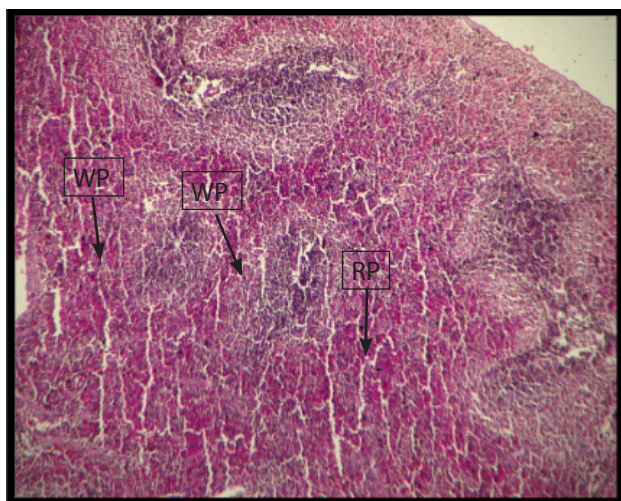


Fig. 5: Normal histological structure of spleen (WP- White pulp and RP- Red pulp) in group 1 and 2 rats (40X)

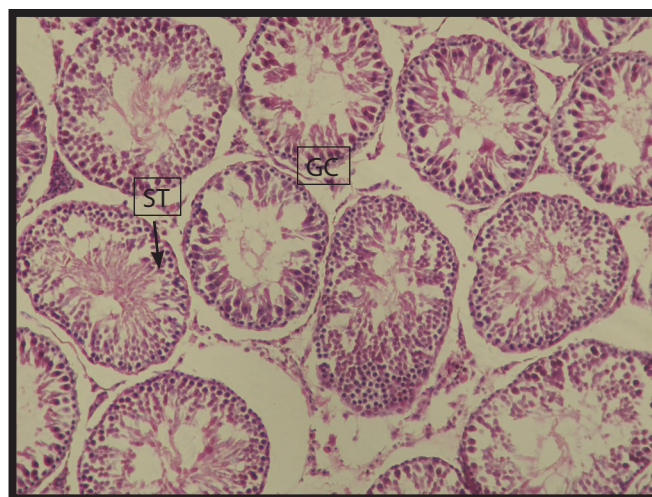


Fig 7: Normal histological structure of testes (ST- Seminiferous tubules, GC-Germinal cells) in group 1 and 2 rats (100X)

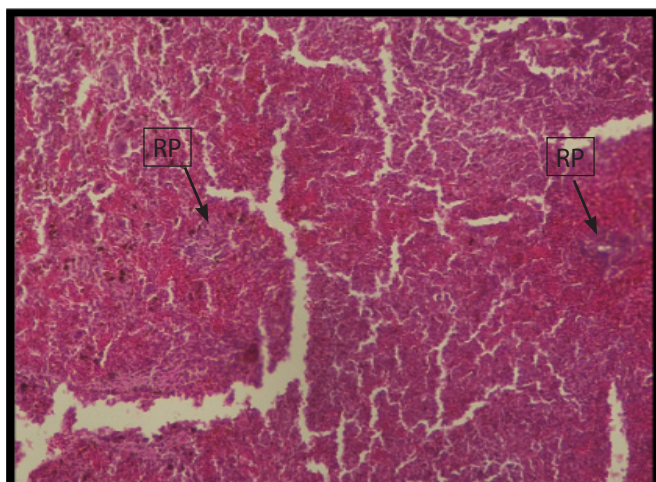


Fig. 6: Depletion of the white pulp in spleen in group 3 rats (RP-Red pulp) (100X)



Fig 8: Loss of germ cells within the lumen of the seminiferous tubules (ST- Seminiferous tubules, GC-Germinal cells) in group 3 rats (100X)

CONCLUSION

The developed iron and zinc nanoparticles having diameters of 100 nm and 71 nm, respectively, demonstrated uniform particle distribution and the formation of stable colloidal systems. The study developed an *in vivo* ideal model of iron deficiency anaemia (IDA) in rats by administering an iron-deficient diet over a period of 8-week, providing a robust framework for subsequent investigations into anaemia and potential therapeutic interventions. Following the establishment of the IDA model, three treatment groups studied revealed acute toxicity in the very high iron & zinc nanoparticle group, leading to 100% mortality within 24 h of first dosing. Subacute toxicity observed over 56 days for the ionic group of iron & zinc, enabled detail assessment of the safety profile of different doses and forms of iron and zinc. Histopathological examination of the liver, kidney, spleen, heart, and testis tissues in the control group and the group

treated with ionic forms of iron and zinc revealed normal structures, whereas significant abnormalities were observed in the group exposed to very high iron (20 mg/d) and zinc (10 mg/d) nanoparticles indicating their adverse effects, requiring further studies.

ACKNOWLEDGEMENT

Authors express their sincere gratitude towards authorities of the College of Veterinary Science and Animal Husbandry, Kamdhenu University, Anand, for providing the financial support and necessary facilities for the successful completion of this work.

REFERENCES

Anonymous (2018). Annual Progress Report 2017-18. Centre of Advanced Research in Plant Tissue Culture. Anand Agricultural University, Anand, Gujarat, India.

- Bhavsar, P.P. (2022). Development of nanofortified functional milk using iron and zinc nanoparticles. *Ph.D. Thesis*. Kamdhenu University, Anand, Gujarat, India.
- Chaparro, C.M., & Suchdev, P.S. (2019). Anaemia: Epidemiology, pathophysiology, and etiology in low-and middle-income countries. *Annals of the New York Academy of Sciences*, 1450(1), 15-31.
- Chen, Y. (2023). The relationship between zinc and human health and how to supplement zinc scientifically. *Theoretical and Natural Science*, 4(1), 1-6.
- Dubey, P., Thakur, V., & Chattopadhyay, M. (2020). Role of minerals and trace elements in diabetes and insulin resistance. *Nutrients*, 12(6), 1-17.
- Ijaz, I., Gilani, E., Nazir, A., & Bukhari, A. (2020). Detail review on chemical, physical and green synthesis, classification, characterizations and applications of nanoparticles. *Green Chemistry Letters and Reviews*, 13(3), 59-81.
- Kulkarni, S., Niharika, S., & Thakur, M. (2020). Sub-acute toxicity assessment of green synthesized hematite nanoparticles (α -Fe₂O₃NPs) using Wistar rat. *Research Journal of Biotechnology*, 15(4), 4.
- Kumar, S., Arora, D., Dhupar, A., Sharma, V., Sharma, J.K., Sharma, S.K., & Gaur, A. (2020). Structural and optical properties of polycrystalline ZnO nanopowder synthesized by direct precipitation technique. *Journal of Nano- and Electronic Physics*, 12(4), 4-27.
- Le, N.T., Truong, N.X., & Dung, D.T. (2022). Green synthesis of iron nanoparticles using *Cleistocalyx operculatus* leaves extract and application iron nanoparticles to treat organic dye Methylene Blue. *Vietnam Journal of Catalysis and Adsorption*, 11(4), 63-67.
- Nahari, M.H., AlAli, A., Asiri, A., Mahnashi, M.H., Shaikh, I.A., Shettar, A.K., & Hoskeri, J. (2022). Green synthesis and characterization of iron nanoparticles synthesized from aqueous leaf extract of *Vitexleucoxylo* *onanditus* biomedical applications. *Nanomaterials*, 12(14), 2404.
- Omar, F.M., Aziz, H.A., & Stoll, S. (2014). Aggregation and disaggregation of ZnO nanoparticles: Influence of pH and adsorption of Suwannee River humic acid. *Science of the Total Environment*, 468, 195-201.
- Ostolska, I., & Wisniewska, M. (2014). Application of the zeta potential measurements to explanation of colloidal Cr₂O₃ stability mechanism in the presence of the ionic polyamino acids. *Colloid and Polymer Science*, 292(10), 2453-2464.
- Prajapati, B.J. (2024). Toxicological and remedial study of zinc nanoparticles and bulk zinc on seed vigour, microbial activity and performance of wheat. *Ph.D. Thesis*. Anand Agricultural University, Anand, Gujarat, India.
- Rehman, N., Jabeen, F., Asad, M., Nijabat, A., Ali, A., Khan, S.U., Luna-Arias, J.P., Mashwani, Z. ur R., Siddiq, A., Karthikeyan, A., & Ahmad, A. (2024). Exposure to zinc oxide nanoparticles induced reproductive toxicities in male Sprague Dawley rats. *Journal of Trace Elements in Medicine and Biology*, 83, 127411.
- Suva, M.A., & Tirgar, P.R. (2023). Comparative evaluation of anti-anaemic effect of sucrosomial iron in experimental model of iron deficiency anaemia in Wistar rats. *Current Issues in Pharmacy and Medical Sciences*, 37(1), 26-32.
- Thakur, M.K., Kulkarni, S., Mohanty, N., Kadam, N., & Swain, N. (2019). Standardization and development of rat model with iron deficiency anaemia utilizing commercial available iron deficient food. *Biosciences, Biotechnology Research Asia*, 16(1), 71-77.
- Tyagi, N., Gupta, P., Khan, Z., Neupane, Y.R., Mangla, B., Mehra, N.,... & Kohli, K. (2023). Superparamagnetic iron-oxide nanoparticles synthesized via green chemistry for the potential treatment of breast cancer. *Molecules*, 28(5), 2343.
- Yun, J.W., Kim, S.H., You, J.R., Kim, W.H., Jang, J.J., Min, S.K., Kim, H.C., Chung, D.H., Jeong, J., Kang, B.C., & Che, J.H. (2015). Comparative toxicity of silicon dioxide, silver and iron oxide nanoparticles after repeated oral administration to rats. *Journal of Applied Toxicology*, 35(6), 681-693.
- Zaman, M., Ang, S., & Singh, S. (2016). Characterizing nanoparticle size by dynamic light scattering. *Journal of the Arkansas Academy of Science*, 70(1), 255-259.
- Zambri, N. D. S., Taib, N. I., Abdul Latif, F., & Mohamed, Z. (2019). Utilization of neem leaf extract on biosynthesis of iron oxide nanoparticles. *Molecules*, 24(20), 3803.

